This article was downloaded by: [Chongqing University]
On: 14 February 2014, At: 13:30
Publisher: Taylor & Francis
Informa Ltd Registered in England and Wales Registered Number: 1072954 Registered office: Mortimer House, 37-41 Mortimer Street, London W1T 3JH, UK

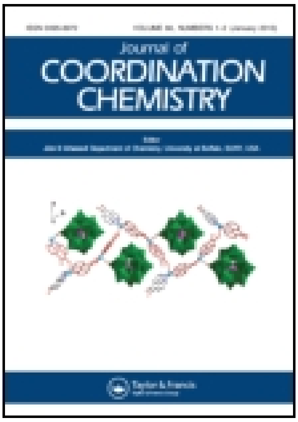

Journal of Coordination Chemistry
Publication details, including instructions for authors and subscription information:
http://www.tandfonline.com/loi/gcoo20

The synthesis, characterization, and theoretical hydrogen gas adsorption properties of copper(II)-3,3′-thiodipropionate complexes with imidazole derivatives

Mürsel Arici[a], Okan Zafer Yeşılel[a], Seda Keskın[b], Onur Şahın[c] & Orhan Büyükgüngör[d]

[a] Department of Chemistry, Faculty of Arts and Sciences, Eskişehir Osmangazi University, Eskişehir, Turkey

[b] Department of Chemical and Biological Engineering, Koç University, İstanbul, Turkey

[c] Scientific and Technological Research Application and Research Center, Sinop University, Sinop, Turkey

[d] Department of Physics, Faculty of Arts and Sciences, Ondokuz Mayıs University, Samsun, Turkey

Accepted author version posted online: 29 Oct 2013.Published online: 04 Dec 2013.

To cite this article: Mürsel Arici, Okan Zafer Yeşılel, Seda Keskın, Onur Şahın & Orhan Büyükgüngör (2013) The synthesis, characterization, and theoretical hydrogen gas adsorption properties of copper(II)-3,3′-thiodipropionate complexes with imidazole derivatives, Journal of Coordination Chemistry, 66:23, 4093-4106, DOI: 10.1080/00958972.2013.860223

To link to this article: http://dx.doi.org/10.1080/00958972.2013.860223

PLEASE SCROLL DOWN FOR ARTICLE

Taylor & Francis makes every effort to ensure the accuracy of all the information (the “Content”) contained in the publications on our platform. However, Taylor & Francis, our agents, and our licensors make no representations or warranties whatsoever as to the accuracy, completeness, or suitability for any purpose of the Content. Any opinions and views expressed in this publication are the opinions and views of the authors, and are not the views of or endorsed by Taylor & Francis. The accuracy of the Content should not be relied upon and should be independently verified with primary sources of information. Taylor and Francis shall not be liable for any losses, actions, claims, proceedings, demands, costs, expenses, damages, and other liabilities whatsoever or howsoever caused arising directly or indirectly in connection with, in relation to or arising out of the use of the Content.

This article may be used for research, teaching, and private study purposes. Any substantial or systematic reproduction, redistribution, reselling, loan, sub-licensing, systematic supply, or distribution in any form to anyone is expressly forbidden. Terms & Conditions of access and use can be found at http://www.tandfonline.com/page/terms-and-conditions

Downloaded by [Chongqing University] at 13:30 14 February 2014

Journal of Coordination Chemistry, 2013
Vol. 66, No. 23, 4093–4106, http://dx.doi.org/10.1080/00958972.2013.860223

Downloaded by [Chongqing University] at 13:30 14 February 2014

The synthesis, characterization, and theoretical hydrogen gas adsorption properties of copper(II)-3,3′-thiodipropionate complexes with imidazole derivatives

MÜRSEL ARICI†, OKAN ZAFER YEŞİLEL*†, SEDA KESKİN‡, ONUR ŞAHİN§ and ORHAN BÜYÜKGÜNGÖR¶

†Department of Chemistry, Faculty of Arts and Sciences, Eskişehir Osmangazi University, Eskişehir, Turkey
‡Department of Chemical and Biological Engineering, Koç University, İstanbul, Turkey
§Scientific and Technological Research Application and Research Center, Sinop University, Sinop, Turkey
¶Department of Physics, Faculty of Arts and Sciences, Ondokuz Mayıs University, Samsun, Turkey

(*Received 4 July 2013; accepted 10 October 2013*)

Three new coordination polymers, $[Cu(\mu_3\text{-tdp})(im)_2]_n$ (**1**), $\{[Cu(\mu_3\text{-tdp})(1\text{-mim})_2]\cdot 0.5H_2O\}_n$ (**2**) and $\{[Cu_2(\mu_3\text{-tdp})_2(4\text{-mim})_4]\cdot H_2O\}_n$ (**3**) [$tdpH_2$ = 3,3′-thiodipropionic acid, im = imidazole, 1-mim = 1-methylimidazole and 4-mim = 4-methylimidazole], have been prepared and characterized by spectroscopic techniques (IR and UV–Vis), elemental analyzes, magnetic measurements, thermal analyzes, and single-crystal X-ray diffraction. Complexes **1–3** crystallize in the monoclinic system with space groups of C2/c and $P2_1/c$, respectively. In **1–3**, tdp is a bridging ligand to form 1-D chains, which are extended into a 2-D layer by hydrogen bonding and $\pi\cdots\pi$ interactions. The 3,3′-thiodipropionate exhibits an unexpected coordination mode in **1–3**. Simulations were used to assess the potential of the complexes in H_2 storage applications.

Keywords: 33′-Thiodipropionic acid; 33′-Thiodipropionate complexes; Imidazole complexes; Copper (II) complexes

1. Introduction

Synthesis and characterization of coordination polymers have attracted interest because of their tunable structure and potential applications in gas adsorption/separation, catalysis, conductivity, magnetism and nonlinear optics [1–9]. The structure of coordination polymer changes depending on organic ligands, metal ions, and supramolecular interactions between organic ligands or metal and organic ligands [10, 11]. The organic ligands play an important role in the determination of the structures of coordination polymers. The most widely used organic ligands in the synthesis of coordination polymers are polycarboxylates, especially dicarboxylates as an anionic ligand and neutral nitrogen-containing ligands owing to their versatile coordination modes [12, 13]. The presence of di, multicarboxylates, and multidentate nitrogen-containing ligands give rise to generation of various frameworks like

---

*Corresponding author. Email: yesilel@ogu.edu.tr

© 2013 Taylor & Francis

Downloaded by [Chongqing University] at 13:30 14 February 2014

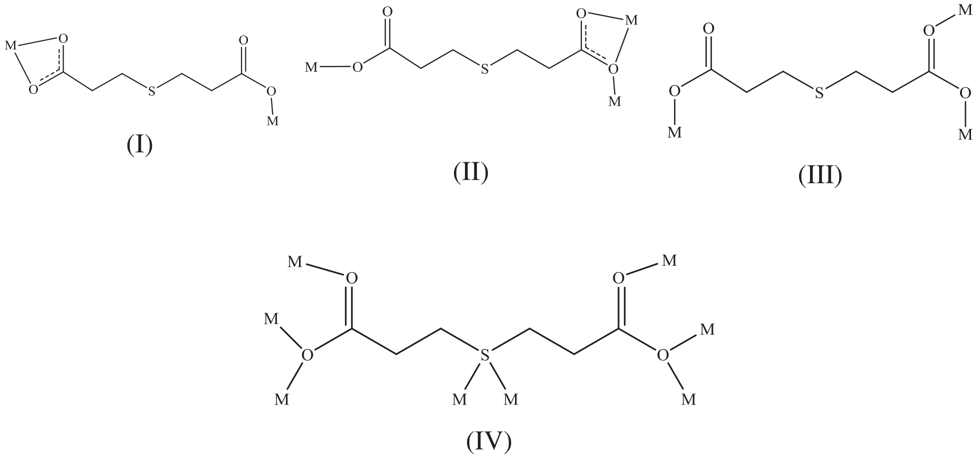

Scheme 1. Coordination modes of 3,3′-thiodipropionate described in the literature.

1-D, 2-D, and 3-D networks in the assembly process [12, 14-16]. Moreover, the noncovalent interactions, such as hydrogen bonding, $\pi \cdots \pi$ stacking and C–H$\cdots\pi$ interactions, play a crucial role in the assembly of polymeric structures [17–19].

So far, although rigid aromatic di, multicarboxylate anions have been widely used in the construction of coordination polymers, flexible aliphatic di, multicarboxylic acids are rarely utilized [20, 21]. However, in recent years, coordination polymers which are synthesized using aliphatic di, multicarboxylic acids which permit structural diversity have been given attention. 3,3′-Thiodipropionic acid (tdpH_2), which is a versatile ligand, is one of the aliphatic dicarboxylic acids and contains five potential donor atoms, four of which come from two carboxylate groups and one of which comes from the thioether group [21]. A few complexes of the tdp ligand with zinc, cadmium, manganese, and silver ions have been synthesized and structurally characterized (scheme 1) [21–24]. In this study, the synthesis, crystal structures, and thermal properties of three new coordination polymers are reported using flexible 3,3′-thiodipropionic acid (H_2tdp). Moreover, molecular simulations were performed to predict theoretical H_2 adsorption in **1–3**.

2. Experimental setup and simulations

2.1. *Materials and measurements*

All chemicals used were analytical reagents and commercially purchased. IR spectra were recorded on a Bruker Tensor 27 FT-IR spectrometer using KBr pellets from 400 to 4000 cm^{-1}. Simultaneous TG, DTG, and DTA analyzes were performed with a Perkin Elmer Diamond TG/DTA Thermal Analyzer under a static air atmosphere with a heating rate of 10 °C min^{-1} in the temperature range 30–800 °C using a platinum pan. Diffraction data for **1** were collected on an Oxford Diffraction Super Nova (single source at offset) Eos diffractometer at 296 K; diffraction data for **2** and **3** were collected at 296 K using a Stoe IPDS diffractometer. In all cases, graphite-monochromated Mo–Kα radiation (λ = 0.71073 Å) was employed. The structures were solved by direct methods using

Downloaded by [Chongqing University] at 13:30 14 February 2014

SHELXS-97 [25] and refined by full-matrix least-squares methods on F^2 using SHELXL-97 [25]. All nonhydrogen atoms were refined anisotropically by full-matrix least-squares methods [25]. Water H atoms were located in a difference map and refined subject to a DFIX restraint of O–H = 0.83(2) Å. Other H atoms were located from different maps and then treated as riding atoms with C–H distances of 0.93–0.97 Å and N–H distances of 0.86 Å. The following procedures were implemented in our analysis: the programs used for molecular graphics were as follow: MERCURY programs [26]; supramolecular analyzes: PLATON [27]; software used to prepare material for publication: WinGX [28]. Elemental analyzes for C, H, N, and S were carried out at the METU Research Center. Magnetic susceptibility measurements were performed using a Sherwood Scientific MXI model Gouy magnetic balance at room temperature. The UV–Vis spectra were obtained using an aqueous solution of the complexes (10^{-3} M) with a Lambda 35 UV–Vis Spectrometer in the range 850–200 nm.

We used Grand Canonical Monte Carlo (GCMC) simulations to predict H_2 adsorption properties of the complexes. Details of GCMC can be found elsewhere [29]. Rigid structures were used and water molecules existing in the pores of **2** and **3** were removed in all simulations. The universal force field (UFF) [30] was used for the framework atoms since previous studies have shown that predictions of GCMC simulation based on UFF for H_2 adsorption in MOFs agree with the experimental measurements [31]. Spherical Lennard–Jones (LJ) 12–6 potentials were used to model H_2 [32]. The Lorentz–Berthelot mixing rules were employed to calculate the adsorbate–adsorbent and adsorbate–adsorbate LJ cross-interaction parameters. Periodic boundary conditions were applied in all simulations and the size of the simulation box was set to 2 × 2 × 2 crystallographic unit cells. Simulations at the lowest fugacity for each system were started from an empty matrix and each subsequent simulation at higher fugacity was started from the final configuration of the previous run. The intermolecular potentials were truncated at 13 Å. Simulations consisted of a total of 1.5×10^7 steps to guarantee the equilibration, followed by 1.5×10^7 steps to sample the desired properties.

2.2. *Synthesis*

2.2.1. $[Cu(\mu_3\text{–tdp})(im)_2]_n$ (1). A mixture of $Cu(OAc)_2 \cdot H_2O$ (1 mmol, 0.200 g) and 3,3′-thiodipropionic acid ($tdpH_2$) (1 mmol, 0.178 g) in water (20 mL) was stirred at 70 °C for an hour and then imidazole (2 mmol, 0.136 g) in water (10 mL) was added to the mixture. The clear solution obtained was stirred at 70 °C for 2 h. The resulting solution was filtered and evaporated at room temperature. Blue crystals were obtained after four days. Yield: 0.215 g, 57% based on $Cu(OAc)_2 \cdot H_2O$. Anal. Calcd for $C_{12}H_{16}N_4O_4SCu$: C, 38.34; H, 4.29; N, 14.91; S, 8.53 %. Found: C, 37.78; H, 4.23; N, 14.70; S, 8.15%. IR (KBr, cm^{-1}): 3352 (m), 3142 (m), 3082 (w), 2968, 2935 (w), 1606 (vs), 1579 (w), 1421 (w), 1369 (vs), 848 (m), 746 (s), 653 (s) cm^{-1}.

2.2.2. $\{[Cu(\mu_3\text{-tdp})(1\text{-mim})_2] \cdot 0.5H_2O\}_n$ (2). Complex **2** was prepared similarly by the method described for the preparation of **1**, with the use of 1-methlyimidazole (2 mmol, 0.164 g) instead of imidazole. Blue crystals of **2** were obtained. Yield: 0.268 g, 63% based on $Cu(OAc)_2 \cdot H_2O$. Anal. Calcd for $C_{14}H_{24}N_4O_5SCu$: C, 39.66; H, 5.71; N, 13.21; S, 7.56%. Found: C, 40.36; H, 4.83; N, 13.39; S, 6.73%. IR (KBr, cm^{-1}): 3474 (br), 3130 (m), 2912 (w), 1618 (vs), 1595 (s), 1522 (w), 1381 (s), 746 (m), 651 (s) cm^{-1}.

2.2.3. $\{[Cu_2(\mu_3\text{-tdp})_2(4\text{-mim})_4]\cdot H_2O\}_n$ (3).

The mixture of 3,3′-thiodipropionic acid (1 mmol, 0.178 g), KOH (2 mmol, 0.112 g), and metallic copper (1 mmol, 0.064 g) was stirred in DMF (10 mL) at 80 °C for two hours. Then, 4-methylimidazole (2 mmol, 0.164 g) in water (20 mL) was added to the mixture and stirred at 80 °C for an hour to obtain a blue solution. After that, the blue solution was filtered to get rid of insoluble particles. Blue crystals of **3** were obtained after about a week and the crystals were collected by filtering and dried at room temperature. Yield: 0.74 g, 89% based on metallic Cu). Anal. Calcd for $C_{28}H_{42}N_8O_9S_2Cu_2$: C, 40.72; H, 5.13; N, 13.57; S, 7.76%. Found: C, 39.34; H, 5.08; N, 13.11; S, 7.38%. IR (KBr, cm^{-1}): 3412 (br), 3134 (m), 3103 (w), 2868 (w), 1608 (vs), 1568 (vs), 1502 (w), 1393 (vs), 827 (m), 652 (s) cm^{-1}.

Downloaded by [Chongqing University] at 13:30 14 February 2014

3. Results and discussion

3.1. *Characterization*

Elemental analysis results of **1–3** are consistent with the proposed formulations. In the IR spectra, for **2** and **3**, broad bands at 3474 and 3412 cm^{-1} show the existence of water in the complexes. For all complexes, the bands observed between 3142 and 3082 cm^{-1} are due to ν(N–H) and aromatic ν(C–H) stretchings. Aliphatic ν(C–H) stretchings are observed between at 2968 and 2868 cm^{-1} for **1–3**. The characteristic asymmetric stretchings corresponding to carboxylate groups are observed at 1606 cm^{-1} for **1**, 1618 cm^{-1} for **2**, and 1608 for **3**. The characteristic bands of carboxylate groups of **1–3** are observed in the range of 1383–1381 cm^{-1} for symmetric stretching. For **1–3**, the Δ values [$\Delta = \nu(COO^-)_{asym} - \nu(COO^-)_{sym}$] are 219, 237, and 215 cm^{-1}, respectively. These Δ values suggest that the coordination mode of the carboxylate groups are probably monodentate bridging [33]. The characteristic thioether (C–S–C) stretching vibrations of **1–3** were observed between 746 and 651 cm^{-1}.

The electronic spectra of **1–3** in water display broad absorption bands at 714 nm (ε = 53.2 L mol^{-1} cm^{-1}), 703 nm (ε = 101.2 L mol^{-1} cm^{-1}), and 731 nm (ε = 92.8 L mol^{-1} cm^{-1}), respectively, which are attributed to $a_1\ (d_z^2) \rightarrow b_1\ (d_{x^2-y^2})$.

Complexes **1–3** exhibit magnetic moment values of 1.60, 1.51, and 1.52 BM, respectively, which correspond to one unpaired electron, lower than the theoretic value of Cu(II) complexes (1.73 BM). These results may be due to antiferromagnetic interaction between adjacent Cu(II) ions in polynuclear copper complexes.

3.2. *Crystal structures*

Details of data collection and crystal structure determinations are given in table 1. Selected bond lengths and angles together with the hydrogen bonding geometry are collected in tables 2 and 3, respectively.

3.2.1. $Cu(\mu_3\text{-tdp})(im)_2]_n$ (1).

The crystal structure of **1** with the atom labeling is shown in figure 1. The asymmetric unit of **1** consists of a Cu(II) ion, two imidazole ligands, and one 3,3′-thiodipropionate (tdp) ligand. The Cu1 exhibits penta-coordination with a distorted square pyramidal geometry. The equatorial coordination comes from two oxygen atoms (O1

Downloaded by [Chongqing University] at 13:30 14 February 2014

Table 1. Crystal data and structure refinement parameters for **1–3**.

Crystal data	**1**	**2**	**3**
Empirical formula	$C_{12}H_{16}CuN_4O_4S$	$C_{28}H_{42}Cu_2N_8O_9S_2$	$C_{28}H_{42}Cu_2N_8O_9S_2$
Formula weight	375.89	825.90	825.90
Crystal system	Monoclinic	Monoclinic	Monoclinic
Space group	C2/c	C2/c	$P2_1/c$
a (Å)	22.267(4)	22.6172(9)	10.0189(9)
b (Å)	16.142(2)	16.9983(7)	18.3006(15)
c (Å)	9.2872(19)	10.0891(4)	19.448(2)
β (°)	111.92(2)	115.415(3)	92.374(8)
V (Å^3)	3096.8(9)	3503.4(2)	3562.8(6)
Z	8	4	4
D_{Calcd} (g cm^{-3})	1.612	1.566	1.540
μ (mm^{-1})	1.57	1.40	1.37
θ Range (°)	3.2–26.3	2.2–27.4	1.5–28.1
Measured reflns.	6633	18,121	7388
Independent reflns.	2992	3633	7388
R_{int}	0.154	0.032	0.000
S	1.04	1.06	1.08
R_1/wR_2	0.147/0.429	0.034/0.079	0.076/0.161
$\Delta\rho_{\max}/\Delta\rho_{\min}$ (eÅ^{-3})	1.81/–1.70	0.28/–0.25	0.45/–0.54

Table 2. Selected bond distances and angles for **1–3** (Å, °).

1					
N1–Cu1	2.027(14)	N3–Cu1	2.030(14)	O1–Cu1	1.959(11)
Cu1–O3^{vi}	1.950(11)	Cu1–O1^{v}	2.478(11)		
O3^{vi}–Cu1–O1	176.1(5)	O3^{vi}–Cu1–N1	90.5(5)	O1–Cu1–N1	90.5(5)
O3^{vi}–Cu1–N3	91.2(5)	O1–Cu1–N3	88.6(5)	N1–Cu1–N3	169.7(5)
O1–Cu1–O1^{v}	80.2(5)	N1–Cu1–O1^{v}	103.0(5)	N3–Cu1–O1^{v}	86.9(4)
2					
N1–Cu1	1.9857(19)	N3–Cu1	1.995(2)	O1–Cu1	1.9834(16)
Cu1–O3^{vii}	1.9838(14)	Cu1–O3^{i}	2.4550(16)		
O1–Cu1–O3^{vii}	173.15(7)	O1–Cu1–N1	91.06(8)	O3^{vii}–Cu1–N1	90.47(7)
O1–Cu1–N3	89.32(8)	O3^{vii}–Cu1–N3	90.09(7)	N1–Cu1–N3	172.14(8)
O1–Cu1–O3^{i}	93.96(6)	N1–Cu1–O3^{i}	95.69(7)	N3–Cu1–O3^{i}	92.11(7)
3					
Cu1–N3	1.969(5)	Cu1–O5	1.983(4)	Cu1–N1	1.986(5)
Cu1–O8^{i}	1.988(4)	Cu2–O1	1.978(4)	Cu2–O3^{vi}	1.980(4)
Cu2–N5	1.983(5)	Cu2–N7	1.999(5)	Cu2–O5	2.418(4)
Cu1–O1	2.447(4)				
N3–Cu1–O5	91.45(18)	N3–Cu1–N1	171.3(2)	O5–Cu1–N1	90.10(19)
N3–Cu1–O8^{i}	90.11(19)	O5–Cu1–O8^{i}	172.05(17)	N1–Cu1–O8^{i}	89.53(19)
N3–Cu1–O1	91.25(17)	N1–Cu1–O1	97.43(17)	O8^{i}–Cu1–O1	95.28(16)
O1–Cu2–O3^{vi}	173.86(17)	O1–Cu2–N5	91.23(18)	O3^{vi}–Cu2–N5	89.0(2)
O1–Cu2–N7	92.59(19)	O3^{vi}–Cu2–N7	88.2(2)	N5–Cu2–N7	169.6(2)
O3^{vi}–Cu2–O5	96.15(16)	N5–Cu2–O5	93.38(18)	N7–Cu2–O5	96.86(18)

Symmetry codes: (v) $-x + 1/2, -y + 1/2, -z + 1$; (vi) $x - 1/2, -y + 1/2, z - 1/2$ for **1**; (i) $-x + 1, y, -z + 3/2$; (vii) $x - 1/2, -y + 3/2, z - 1/2$ for **2**; (i) $x, -y + 1/2, z + 1/2$; (vi) $x, -y + 1/2, z - 1/2$ for **3**.

and O3^{vi}) of two different tdp ligands and two nitrogen atoms (N1 and N3) of two different im ligands, while the apical position is occupied by oxygen atom (O1^{v}) of tdp ligand ((v) $-x + 1/2, -y + 1/2, -z + 1$; (vi) $x - 1/2, -y + 1/2, z - 1/2$). According to the Addison definition, the value of τ for Cu1 is 0.105 ($\tau = 0$ for an ideal square pyramid, $\tau = 1$ for an ideal trigonal bipyramid) [34]. The Cu–N bond lengths are 2.027(14) and 2.030(14) Å and

Downloaded by [Chongqing University] at 13:30 14 February 2014

Table 3. C–H···Cu interactions and hydrogen bond parameters for **1–3** (Å, °).

D–H···A	D–H	H···A	D···A	D–H···A
1				
N4–H4···O4^{i}	0.86	2.09	2.925(18)	165
C2–H2A···O3^{ii}	0.97	2.56	3.469(19)	156
C8–H8···O2^{iii}	0.93	2.51	3.17(2)	128
C11–H11···O2^{iv}	0.93	2.58	3.28(2)	133
2				
O5–H5A···O2^{i}	0.82(2)	2.13(3)	2.911(3)	158(5)
C4–H4A···O2^{ii}	0.96	2.49	3.416(4)	162
C4–H4C···O4^{iii}	0.96	2.45	3.362(4)	160
C8–H8C···O4^{iv}	0.96	2.55	3.448(4)	156
C13–H13B···O1^{i}	0.97	2.53	3.293(3)	135
C6–H6···O2^{v}	0.93	2.49	3.308(3)	147
3				
N6–H6A···O7^{ii}	0.86	2.12	2.958(7)	166
N4–H4···O4^{iii}	0.86	1.97	2.815(6)	167
N2–H2A···O9	0.86	1.96	2.816(7)	177
O9–H9B···O4	0.84(2)	2.05(5)	2.803(7)	148(8)
O9–H9A···O7^{ii}	0.84(2)	1.95(2)	2.785(7)	173(10)
C2–H2···O6	0.93	2.58	3.208(8)	125
C8–H8A···O2^{iv}	0.96	2.42	3.282(9)	150
C12–H12C···O6^{v}	0.96	2.43	3.374(10)	167
C18–H18B···O8^{i}	0.97	2.58	3.413(8)	144
C27–H27A···Cg1	0.97	3.185	4.028	146

Symmetry codes: (i) $-x + 1, y, -z + 1/2$; (ii) $-x + 1, y, -z + 3/2$; (iii) $x, -y + 1, z + 1/2$; (iv) $-x + 1/2, -y + 1/2, -z$ for **1**; (i) $-x + 1, y, -z + 3/2$; (ii) $x, -y + 1, z-1/2$; (iii) $x-1/2, y-1/2, z-1$; (iv) $-x + 1, -y + 2, -z + 2$; (v) $-x + 1/2, -y + 3/2, -z + 2$ for **2**; (i) $x, -y + 1/2, z + 1/2$; (ii) $x + 1, -y + 1/2, z + 1/2$; (iii) $x - 1, -y + 1/2, z - 1/2$; (iv) $x - 1, y, z$; (v) $x + 1, y, z$ for **3**.

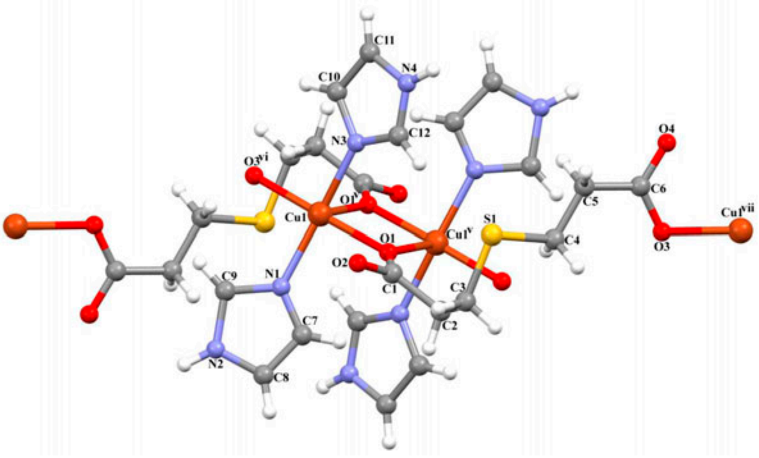

Figure 1. The molecular structure of **1** showing the atom numbering scheme ((v) $-x + 1/2, -y + 1/2, z + 1$; (vi) $1 - x, y, 1.5 - z$; (vii) $-x, y, ½ - z$).

the Cu–O bond lengths are 1.950(11), 1.959(11), and 2.478(11) Å, respectively. O1^{v} of the tdp ligand is weakly coordinated to the Cu(II) ion and longer than those of the equatorial Cu–O bonds ((v) $-x + 1/2, -y + 1/2, -z + 1$). These values are comparable to those observed in other Cu(II) complexes with imidazole ligand [35–39]. The tdp ligand displays

Downloaded by [Chongqing University] at 13:30 14 February 2014

an unprecedented μ_3-coordination mode in **1**. The Cu(II) ions are doubly bridged by tdp ligands to generate helical-like polymeric chains with 20-membered rings. These 20-membered rings are produced by two tdp ligand atoms and two Cu(II) ions (figure 2). One of the O atoms (O1 and $O1^{v}$) of two tdp ligands acts as a bridge to connect two Cu(II) ions, thus forming a rhomboidal Cu_2O_2 ring. Adjacent Cu_2O_2 binuclear motifs are further joined by the tdp ligands through carboxyl atoms, generating 1-D coordination polymer, with the $Cu1\cdots Cu1^{v}$ and $Cu1\cdots Cu1^{vii}$ separations of 3.410 Å and 8.104 Å ((v) $-x + 1/2$, $-y + 1/2$, $-z + 1$; (vii) $-x$, y, $1/2 - z$) (figure 2). The imidazole rings are almost planar, maximum deviations from the least-squares planes being 0.0267(10) Å for C8 and 0.0116 (10) Å for C10.

An intermolecular $\pi\cdots\pi$ contact occurs between the two symmetry-related imidazole rings of neighboring molecules. Cg1 is oriented in such a way that the perpendicular distance from Cg1 to $Cg1^{iv}$ is 3.180 Å ((iv) $-x + 1/2$, $-y + 1/2$, $-z$). The distance between the ring centroids is 3.406 Å. N4 in the molecule at (x, y, z) acts as a hydrogen-bond donor, via H4 to O4 at ($-x + 1$, y, $-z + 1/2$), so forming a centrosymmetric R_2^2 ring. The 1-D layer is extended into 2-D frameworks by π–π interactions and N–H···O hydrogen bonds (figure 2). C8 in the imidazole ligand at (x, y, z) acts as a hydrogen-bond donor, via H8, to O2 at (x, $-y + 1$, $z + 1/2$), so forming a C(8) chain running parallel to the [001] direction. C2 and C11 in the molecule at (x, y, z) act as hydrogen-bond donors, via H2A and H11, respectively, to O3 at ($-x + 1$, y, $-z + 3/2$) and O2 at ($-x + 1/2$, $-y + 1/2$, $-z$), so forming centrosymmetric $R_2^2 16$ rings. The intermolecular C–H···O hydrogen bonds play a crucial role in the architecture of the 3-D network (figure 3).

3.2.2. {[Cu(μ_3-tdp)(1-mim)$_2$]·0.5H$_2$O}$_n$ (2).

The molecular structure of **2** with the atom labeling is shown in figure 4. The asymmetric unit of **2** consists of a Cu(II) ion, two 1-methylimidazole (1-Mim) ligands, one tdp ligand, and one half noncoordinated water molecule. The water atom lies in a special position. The Cu1 atom displays a CuN_2O_3

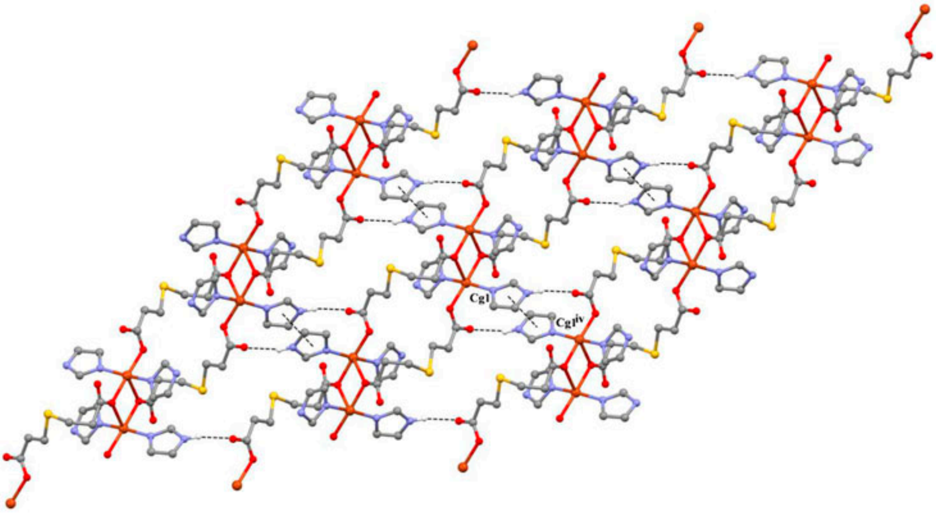

Figure 2. An infinite 2-D layer of **1**.

Downloaded by [Chongqing University] at 13:30 14 February 2014

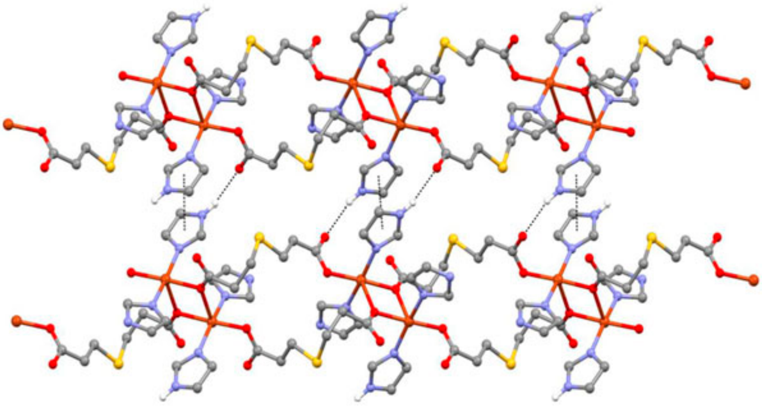

Figure 3. The C–H···O hydrogen bonds of **1**.

square pyramidal geometry. The equatorial plane has two oxygen atoms (O1 and O3^{vii}) of two different tdp ligands and two nitrogen atoms (N1 and N3) of two 1-mim ligands, while the apical position is occupied by oxygen atom (O3^{i}) of tdp ligand ((i) $-x + 1$, y, $-z + 3/2$; (vii) $x - 1/2$, $-y + 3/2$, $z - 1/2$). The value of τ for Cu1 is 0.017, indicating that the square pyramidal coordination geometry has no significant distortion. The Cu–O bond lengths are 1.9834(16), 1.9838(14), and 2.4550(16) Å and the Cu–N bond lengths are 1.9857(19) and 1.995(2) Å, respectively. The Cu1-O3^{i} distance (2.4550(16) Å) is longer than the corresponding distances in related structures. All these bonding parameters are comparable to those observed in other Cu(II) complexes with imidazoles [40–44]. Adjacent 20-membered rings are further joined by the rhomboidal Cu_2O_2 rings, generating 1-D coordination polymer running parallel to the [101] direction. The Cu1···Cu1^{viii} and Cu1···Cu1^{i} separations are 3.432 Å and 8.210 Å ((viii) $-x + 1/2$, $-y + 3/2$, $-z + 1$) (figure 5). The imidazole rings are almost planar, maximum deviations from the least-squares planes being 0.0112(20) Å for N2 and 0.0051(16) Å for C7.

In **2**, $\pi \cdots \pi$ interaction exists between the two symmetry-related imidazole rings of neighboring molecules. The perpendicular distance from Cg1 to Cg1^{v} is 3.430 Å ($-x + 1/2$, $-y + 3/2$, $-z + 2$). Adjacent 1-D chains are connected by $\pi \cdots \pi$ interactions and O–H···O hydrogen bonds to form 2-D supramolecular network (figure 5). C8 in the molecule at (x, y, z) acts as a hydrogen-bond donor, via H8C to O4 at ($-x + 1$, $-y + 2$, $-z + 2$), so forming a centrosymmetric $R_2^2$30 ring centered at (0, 1, 1). Similarly, C6 in the molecule at (x, y, z) acts as a hydrogen-bond donor, via H6 to O2 at ($-x + 1/2$, $-y + 3/2$, $-z + 2$), so forming a centrosymmetric τ ring centered at (1/4, 3/4, 1). C4 in the molecule at (x, y, z) acts as a hydrogen-bond donor, via H4A and H4C, to O2 at (x, $-y + 1$, $z - 1/2$) and O4 at ($x - 1/2$, $y - 1/2$, $z - 1$), so forming C(9) and C(15) chains running parallel to the [001] and [111] directions. These C–H···O hydrogen bonds play a crucial role in the architecture of the 3-D network (figure 6).

3.2.3. {[Cu_2(μ_3-tdp)$_2$(4-mim)$_4$]·H_2O}$_n$ (3).

The crystal structure of **3** with the atom labeling is shown in figure 7. The asymmetric unit of **3** consists of two Cu(II) ions, four 4-methylimidazole ligands, two tdp ligands, and one noncoordinated water molecule. Each

Downloaded by [Chongqing University] at 13:30 14 February 2014

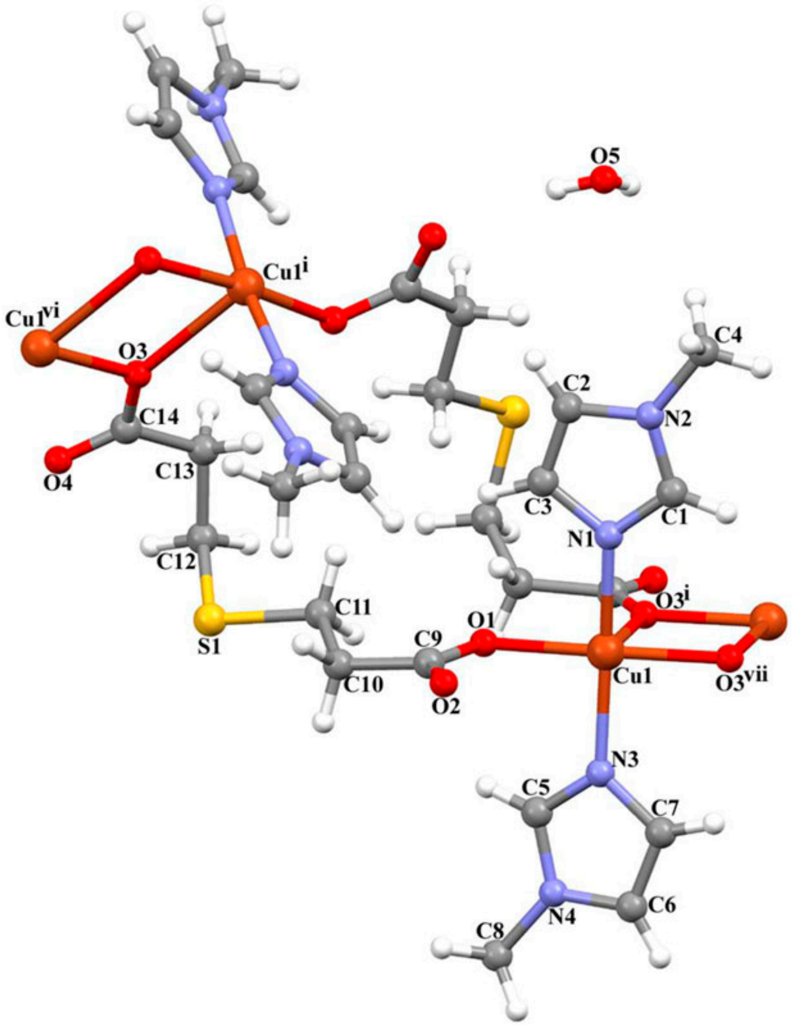

Figure 4. The molecular structure of **2** showing the atom numbering scheme ((i) $-x + 1$, y, $-z + 3/2$; (vi) $1/2 - x$, $1.5 - y$, $1 - z$; (vii) $x - 1/2$, $-y + 3/2$, $z - 1/2$).

Cu(II) ion exhibits square pyramidal geometry. Each Cu(II) ion is coordinated by three oxygen atoms from three different tdp ligands and two nitrogen atoms from two different 4-methylimidazole ligands. The values of τ for Cu1 and Cu2 are 0.013 and 0.071, respectively, indicating that the two square pyramidal coordination geometries have no significant distortion [34]. The Cu–O bond distances range between 1.978(4) and 2.447 (4) Å. The Cu1–O1 and Cu2–O5 distances (2.447(4) and 2.418(4) Å) are longer than the other equatorial Cu–O bonds [45, 46]. The Cu–N bond distances range between 1.969(5) and 1.999(5) Å, which is typical in Cu(II) complexes with the 4-methylimidazole ligand [37, 47–49]. The two Cu(II) ions and two tdp ligands generate a rhomboidal Cu_2O_2 ring and a 20-membered ring. The combination of Cu_2O_2 rings and 20-membered rings produce a 1-D coordination polymer running parallel to the [001] direction. The Cu1···Cu2 and

Downloaded by [Chongqing University] at 13:30 14 February 2014

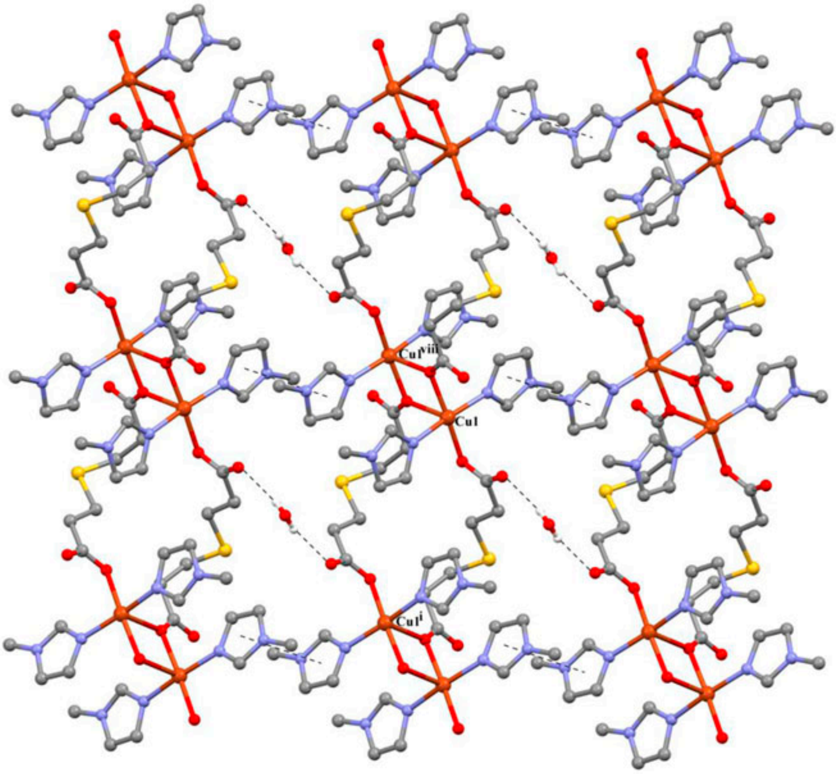

Figure 5. An infinite 2-D layer of **2** ((i) –*x* + 1, *y*, –*z* + 3/2).

Cu1···Cu2^{i} separations are 3.454 Å and 7.615 Å ((i) *x*, –*y* + 1/2, *z* + 1/2) (figure 8), respectively. The imidazole rings are almost planar, maximum deviations from the least-squares planes being 0.0037(38) Å for C1, 0.0036(36) Å for N3, 0.0029(37) Å for N6, and 0.0135(61) Å for C13.

N4 and N6 in the molecule at (x, y, z) act as hydrogen-bond donors, via H4 and H6A, respectively, to O4 at (*x* – 1, –*y* + 1/2, *z* – 1/2) and O7 at (*x* + 1, –*y* + 1/2, *z* + 1/2), so forming C(14) $R_2^2 28$ chains running parallel to the [101] direction. The packing diagram of **3** contains a 2-D layer filled with crystal water molecules (figure 8). C8 and C12 in the molecule at (*x*, *y*, *z*) act as hydrogen-bond donors, via H8A and H12C, respectively, to O2 at (*x* – 1, *y*, *z*) and O6 at (*x* + 1, *y*, *z*), so forming C(9) $R_2^2 18$ chains of rings running parallel to the [100] direction.

3.3. *Thermal properties*

The thermal stabilities and thermal decomposition behaviors of **1–3** were studied by thermal analysis in a static air atmosphere from 30 to 800 °C, as shown in figures S1–S3. Complex **1** is stable to 165 °C. For **2** and **3**, the first weight losses of 2.06% from 40 to 151 °C and 1.99% from 81 to 146 °C correspond to the release of lattice water molecules, respectively. The most significant weight losses of 59.98% (Calcd 59.86%) from 165 to 278 °C for **1**,

Downloaded by [Chongqing University] at 13:30 14 February 2014

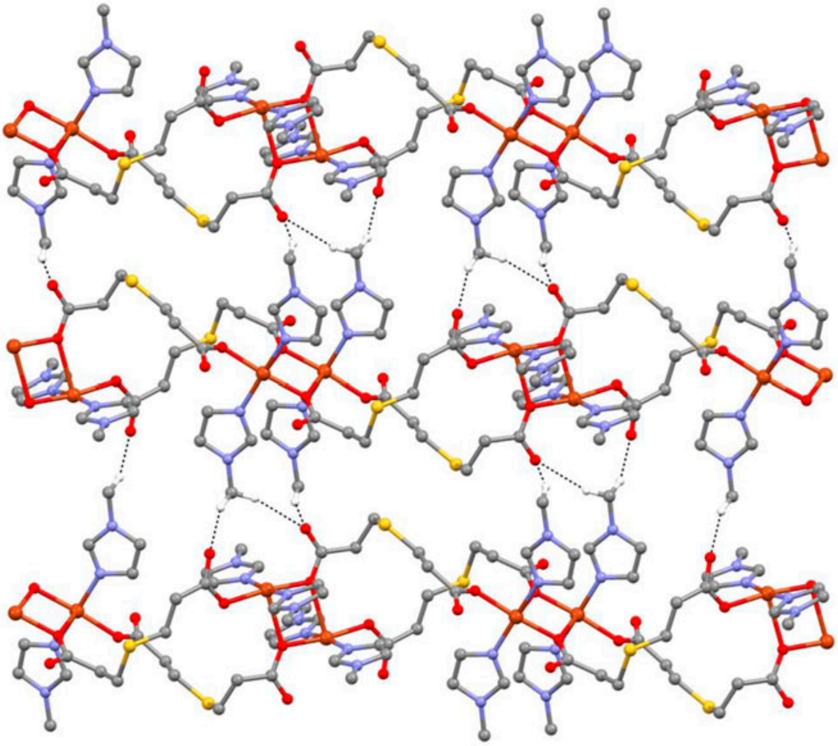

Figure 6. The C–H···O hydrogen bonds of **2**.

63.30% (Calcd 61.30%) from 152 to 313 °C for **2,** and 61.44% (Calcd 61.30%) from 146 to 279 °C for **3** with endothermic and exothermic peaks correspond to the removal of neutral ligands, respectively. Moreover, the tdp ligand starts to decompose in the temperature range of above temperatures. On further heating, the final residual products of **1–3** with weight losses of 21.62% for **1**, 21.20% for **2,** and 17.80% for **3** are possibly CuO (Calcd 21.25% for **1**, 19.25% for **2,** and 19.25% for **3**) with complete decomposition.

3.4. *Computational details*

Figure 9 shows the simulated H_2 adsorption capacities of **1–3** at 77 K and 298 K as a function of pressure. As expected, the adsorbed H_2 amount increases with presssure and decreases with temperature. All the complexes are away from the saturation except the adsorption isotherms of **2** at 77 K which reaches saturation quickly. The differences between the H_2 isotherm results can be attributed to the pore sizes of the complexes. Complex **2** has a pore size around 3 Å whereas the pore sizes of **1** and **3** are around 2.7 and 2.6 Å, respectively. Therefore, it is reasonable to see higher H_2 adsorption in **2**. These pore sizes are smaller than the kinetic diameter of the CH_4 molecule. Therefore, these complexes can be used as molecular sieves to separate H_2 from CH_4.

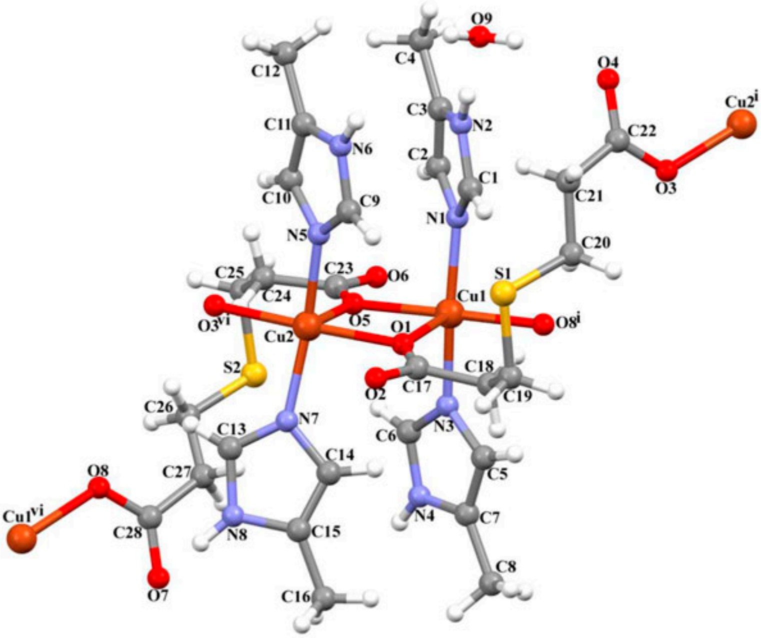

Figure 7. The molecular structure of **3** showing the atom numbering scheme ((i) $x, -y + 1/2, z + 1/2$; (vi) $x, -y + 1/2, z - 1/2$).

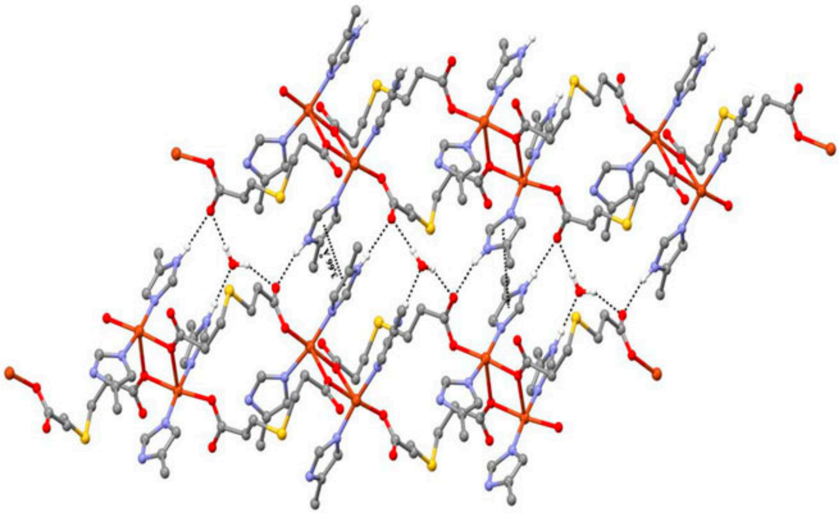

Figure 8. Complex **3** and water link neighboring polymeric chains via O–H···O and N–H···O hydrogen bonds into a 2-D framework parallel to the [101] direction.

Downloaded by [Chongqing University] at 13:30 14 February 2014

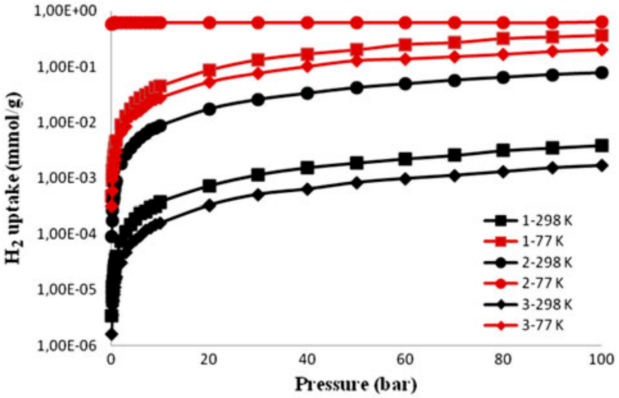

Figure 9. Simulated H_2 uptake capacities of **1**–**3** at 77 and 298 K.

4. Conclusion

Three new Cu(II)-3,3′-thiodipropionate coordination polymers were synthesized and characterized. The tdp exhibits a new coordination mode and acts as a bridging ligand to form a 1-D chain, which is extended into a 3-D supramolecular network by hydrogen bonding, $\pi\cdots\pi$ and C–H$\cdots\pi$ interactions in **1–3**. Molecular simulations show that H_2 storage capacities of **1–3** increase as temperature decreases and **1–3** can be proposed as molecular sieves to separate H_2 from CH_4.

Supplementary material

Crystallographic data for the structural analysis have been deposited with the Cambridge Crystallographic Data Center, CCDC No. 932988 for **1**, 932989 for **2,** and 932990 for **3**. Copies of this information may be obtained free of charge from the Director, CCDC, 12 Union Road, Cambridge CB2 1EZ, UK (Fax: +44–1223-336,033; E-mail: deposit@ccdc.cam.ac.uk or www: http://www.ccdc.cam.ac.uk).

Acknowledgement

This work was supported by the Scientific Research Fund of Eskişehir Osmangazi University [Project number 201219A101].

Supplemental data

Supplemental data for this article can be accessed http://dx.doi.org/10.1080/00958972.2013.860223.

References

[1] S. Kitagawa, R. Kitaura, S.I. Noro. *Angew. Chem. Int. Ed.*, **43**, 2334 (2004).
[2] N.L. Rosi, J. Eckert, M. Eddaoudi, D.T. Vodak, J. Kim, M. O’Keeffe, O.M. Yaghi. *Science*, **300**, 1127 (2003).

Downloaded by [Chongqing University] at 13:30 14 February 2014

[3] H. Li, M. Eddaoudi, M. O'Keeffe, O.M. Yaghi. *Nature*, **402**, 276 (1999).
[4] M. Eddaoudi, J. Kim, N. Rosi, D. Vodak, J. Wachter, M. O'Keeffe, O.M. Yaghi. *Science*, **295**, 469 (2002).
[5] D. Farrusseng, S. Aguado, C. Pinel. *Angew. Chem. Int. Ed.*, **48**, 7502 (2009).
[6] S. Hasegawa, S. Horike, R. Matsuda, S. Furukawa, K. Mochizuki, Y. Kinoshita, S. Kitagawa. *J. Am. Chem. Soc.*, **129**, 2607 (2007).
[7] Y. Cui, O.R. Evans, H.L. Ngo, P.S. White, W. Lin. *Angew. Chem. Int. Ed.*, **41**, 1159 (2002).
[8] J.L.C. Rowsell, O.M. Yaghi. *Angew. Chem. Int. Ed.*, **44**, 4670 (2005).
[9] M. O'Keeffe, M. Eddaoudi, H. Li, T. Reineke, O.M. Yaghi. *J. Solid State Chem.*, **152**, 3 (2000).
[10] G.L. Wen, Y.Y. Wang, W.H. Zhang, C. Ren, R.T. Liu, Q.Z. Shi. *Cryst. Eng. Comm.*, **12**, 1238 (2010).
[11] D. Sun, G.G. Luo, N. Zhang, J.H. Chen, R.B. Huang, L.R. Lin, L.S. Zheng. *Polyhedron*, **28**, 2983 (2009).
[12] X. Guo, X. Li, X. Weng, S. Lin. *J. Mol. Struct.*, **1008**, 63 (2012).
[13] H. Park, A.J. Lough, J.C. Kim, M.H. Jeong, Y.S. Kang. *Inorg. Chim. Acta*, **360**, 2819 (2007).
[14] H. He, F. Dai, A. Xie, X. Tong, D. Sun. *Cryst. Eng. Comm*, **10**, 1429 (2008).
[15] S.K. Dey, B. Bag, K. Abdul Malik, M.S. El Fallah, J. Ribas, S. Mitra. *Inorg. Chem.*, **42**, 4029 (2003).
[16] T. Fukushima, S. Horike, Y. Inubushi, K. Nakagawa, Y. Kubota, M. Takata, S. Kitagawa. *Angew. Chem. Int. Ed.*, **49**, 4820 (2010).
[17] A. Grirrane, A. Pastor, E. Álvarez, C. Mealli, A. Ienco, D. Masi, A.N. Galindo. *Inorg. Chem. Commun.*, **8**, 463 (2005).
[18] G. Guilera, J.W. Steed. *Chem. Commun.*, **1563**, (1999).
[19] T. Duangthongyou, S. Jirakulpattana, C. Phakawatchai, M. Kurmoo, S. Siripaisarnpipat. *Polyhedron*, **29**, 1156 (2010).
[20] Y.Q. Zheng, J.L. Lin, W. Xu, H.Z. Xie, J. Sun, X.W. Wang. *Inorg. Chem.*, **47**, 10280 (2008).
[21] P.P. Yang, B. Li, Y.H. Wang, W. Gu, X. Liu. *Z. Anorg. Allg. Chem.*, **634**, 1221 (2008).
[22] A. Grirrane, E. Álvarez, A. Pastor, A. Galindo. *Z. Anorg. Allg. Chem.*, **636**, 2409 (2010).
[23] Y.-H. Liu, B. Li, X. Liu. *Chin. J. Chem.*, **10**, 034 (2009).
[24] M. Arıcı, O.Z. Yeşilel, S. Keskin, M. Taş. *Polyhedron*, **45**, 103 (2012).
[25] G.M. Sheldrick. *Acta Cryst.*, **A64**, 112 (2008).
[26] C.F. Macrae, P.R. Edgington, P. McCabe, E. Pidcock, G.P. Shields, R. Taylor, M. Towler, J. Streek. *J. Appl. Crystallogr.*, **39**, 453 (2006).
[27] A.L. Spek. *PLATON A Multipurpose Crystallographic Tool.*, Utrecht University, Utrecht (2001).
[28] L.J. Farrugia. *J. Appl. Crystallogr.*, **32**, 837 (1999).
[29] D. Frenkel, B. Smit. *Understanding Molecular Simulation: From Algorithms to Applications*, 2nd Edn., Academic Press, San Diego, CA (2002).
[30] A.K. Rappe, C.J. Casewit, K.S. Colwell, W.A. Goddard, W.M. Skiff. *J. Am. Chem. Soc.*, **114**, 10024 (1992).
[31] S. Keskin, J. Liu, R.B. Rankin, J.K. Johnson, D.S. Sholl. *Ind. Eng. Chem. Res.*, **48**, 2355 (2009).
[32] V. Buch. *J. Chem. Phys.*, **100**, 7610 (1994).
[33] K. Nakamoto. *Infrared and Raman Spectra of İnorganic and Coordination Compounds. Part A, Theory and Applications in İnorganic Chemistry.*, Wiley, New York, NY (1997).
[34] A.W. Addison, T.N. Rao, J. Reedijk, J.V. Rijn, G.C. Verschoor. *J. Chem. Soc., Dalton Trans.* (1984).
[35] I.O. Fritsky, J.Ś. Kozłowska, A. Dobosz, T.Y. Sliva, N.M. Dudarenko. *Inorg. Chim. Acta*, **357**, 3746 (2004).
[36] H.-Y. Bie, J.-H. Yu, J.-Q. Xu, J. Lu, Y. Li, X.-B. Cui, X. Zhang, Y.-H. Sun, L.-Y. Pan. *J. Mol. Struct.*, **660**, 107 (2003).
[37] A.T. Çolak, F. Çolak, D. Akduman, O.Z. Yeşilel, O. Büyükgüngör. *Solid State Sci.*, **11**, 1908 (2009).
[38] X.-C. Fu, X.-Y. Wang, M.-T. Li, C.-G. Wang, X.-T. Deng. *Acta Crystallogr., Sect. C: Cryst. Struct. Commun.*, **62**, m343 (2006).
[39] B.D. Wu, S.W. Wang, L. Yang, T.L. Zhang, J.G. Zhang, Z.N. Zhou, KBYu Eur. *J. Inorg. Chem.*, **2011**, 2616 (2011).
[40] S.G. Baca, I.G. Filippova, O.A. Gherco, M. Gdaniec, Y.A. Simonov, N.V. Gerbeleu, P. Franz, R. Basler, S. Decurtins. *Inorg. Chim. Acta*, **357**, 3419 (2004).
[41] J. Castro, P. Perez-Lourido, A. Sousa-Pedrares, E. Labisbal, M. Carabel, J.A. Vazquez. *Acta Crystallogr., Sect. C: Cryst. Struct. Commun.*, **58**, m65 (2002).
[42] S.X. Yan, D. Zhao, T. Li, R. Wang, X.R. Meng. *J. Coord. Chem.*, **65**, 945 (2012).
[43] M. Pi, T. Wang, C.M. Jin. *J. Coord. Chem.*, **64**, 600 (2011).
[44] H.L. Wen, T.T. Wang, C.B. Liu, M. He, Y.X. Wang. *J. Coord. Chem.*, **65**, 856 (2012).
[45] S.M. Hu, S.C. Xiang, J.J. Zhang, T.L. Sheng, R.B. Fu, XTWu Eur. *J. Inorg. Chem.*, **1141**, (2008).
[46] Y. Song, P. Gamez, A.F. Stassen, M. Lutz, A.L. Spek, J. Reedijk. *Eur. J. Inorg. Chem.*, **4073**, (2003).
[47] C. Nather, M. Wriedt, I. Jess. *Acta Crystallogr., Sect. E: Struct. Rep. Online*, **58**, m107 (2002).
[48] H.-Y. Wang, S.-J. Liu, R.-J. Wang, C.-C. Su. *Acta Crystallogr., Sect. C: Cryst. Struct. Commun.*, **59**, m512 (2003).
[49] O.Z. Yeşilel, İ. İlker, O. Büyükgüngör. *Polyhedron*, **28**, 3010 (2009).

Downloaded by [Chongqing University] at 13:30 14 February 2014